

**This item is the archived peer-reviewed author-version of:**

The drivers of dark diversity in the Scandinavian mountains are metric-dependent

**Reference:**

Hostens Lore, Van Meerbeek Koenraad, Wiegmans Dymphna, Larson Keith, Lenoir Jonathan, Clavel Jan, Wedegärtner Ronja, Pirée Amber, Nijs Ivan, Lembrechts Jonas.- The drivers of dark diversity in the Scandinavian mountains are metric-dependent  
Journal of vegetation science - ISSN 1654-1103 - 34:6(2023), e13212  
Full text (Publisher's DOI): <https://doi.org/10.1111/JVS.13212>  
To cite this reference: <https://hdl.handle.net/10067/2005620151162165141>

1 **The drivers of dark diversity in the Scandinavian mountains are metric-dependent**

2 *Hostens Lore<sup>1</sup>, Van Meerbeek Koenraad<sup>2,3</sup>, Wiegmans Dymphna<sup>1</sup>, Larson Keith<sup>4</sup>, Lenoir Jonathan<sup>5</sup>,*  
3 *Clavel Jan<sup>1</sup>, Wedegärtner Ronja<sup>6</sup>, Pirée Amber<sup>1</sup>, Nijs Ivan<sup>1</sup>, Lembrechts J. Jonas<sup>1</sup>*

4 Short title: Dark diversity can be metric-dependent

5 **Affiliations**

6 <sup>1</sup>Research Group Plants and Ecosystems (PLECO), University of Antwerp, Belgium

7 <sup>2</sup>Department Earth of Environmental Science, KU Leuven, Leuven, Belgium

8 <sup>3</sup>KU Leuven Plant Institute, KU Leuven, Leuven, Belgium

9 <sup>4</sup>Climate Impacts Research Centre, Department of Ecology and Environmental Sciences, Umeå  
10 University, Sweden

11 <sup>5</sup>UMR CNRS 7058, Ecologie et Dynamique des Systèmes Anthropisés (EDYSAN), Université de Picardie  
12 Jules Verne, Amiens, France

13 <sup>6</sup>Department of Biology, Norwegian University of Science and Technology, Trondheim, Norway

14 **Correspondence**

15 Lore Hostens, Research Group Plants and Ecosystems (PLECO), University of Antwerp, Belgium

16 Email: lore.hostens@kuleuven.be

17 Orcid: <https://orcid.org/0000-0001-8245-1152>

18 Jonas J. Lembrechts, Research Center Plants and Ecosystems (PLECO), University of Antwerp, Belgium

19 Email: jonas.lembrechts@uantwerpen.be

20 Orcid: <https://orcid.org/0000-0002-1933-0750>

21 **Funding information**

22 This project was funded by FWO projects G018919N, 12P1819N and W001919N, as well as by ANR-20-  
23 EBIS-0004, BiodivERsA, BiodivClim call 2019–2020.

24 **Abstract**

25 **Aim:** Dark diversity refers to the set of species that are not observed in an area but could potentially  
26 occur based on suitable local environmental conditions. In this paper, we applied both niche-based  
27 and co-occurrence-based methods to estimate the dark diversity of vascular plant species in the  
28 subarctic mountains. We then aimed to unravel the drivers explaining (1) why some locations were  
29 missing relatively more suitable species than others, and (2) why certain plant species were more often  
30 absent from suitable locations than others.

31 **Location:** The Scandinavian mountains around Abisko, northern Sweden.

32 **Methods:** We calculated the dark diversity in 107 plots spread out across four mountain trails using  
33 four different methods. Two co-occurrence-based (Beals' index and hypergeometric method) and two  
34 niche-based (climatic niche model and climatic niche model followed by species-specific threshold)  
35 methods. This was then followed by multiple generalized linear mixed-effects models and general  
36 linear models to determine which habitat characteristics and species traits contributed the most to  
37 dark diversity.

38 **Results:** The study showed a notable divergence in the predicted drivers of dark diversity depending  
39 on the method used. Nevertheless, we can conclude that plot-level dark diversity was generally 17%  
40 higher in areas at low elevations and 31% higher in areas with a low species richness.

41 **Conclusion:** Our findings call for caution when interpreting statistical findings of dark diversity  
42 estimates. Even so, all analyses point towards an important role for natural processes such as

43 competitive dominance as the main driver of the spatial patterns found in dark diversity in the  
44 northern Scandes.

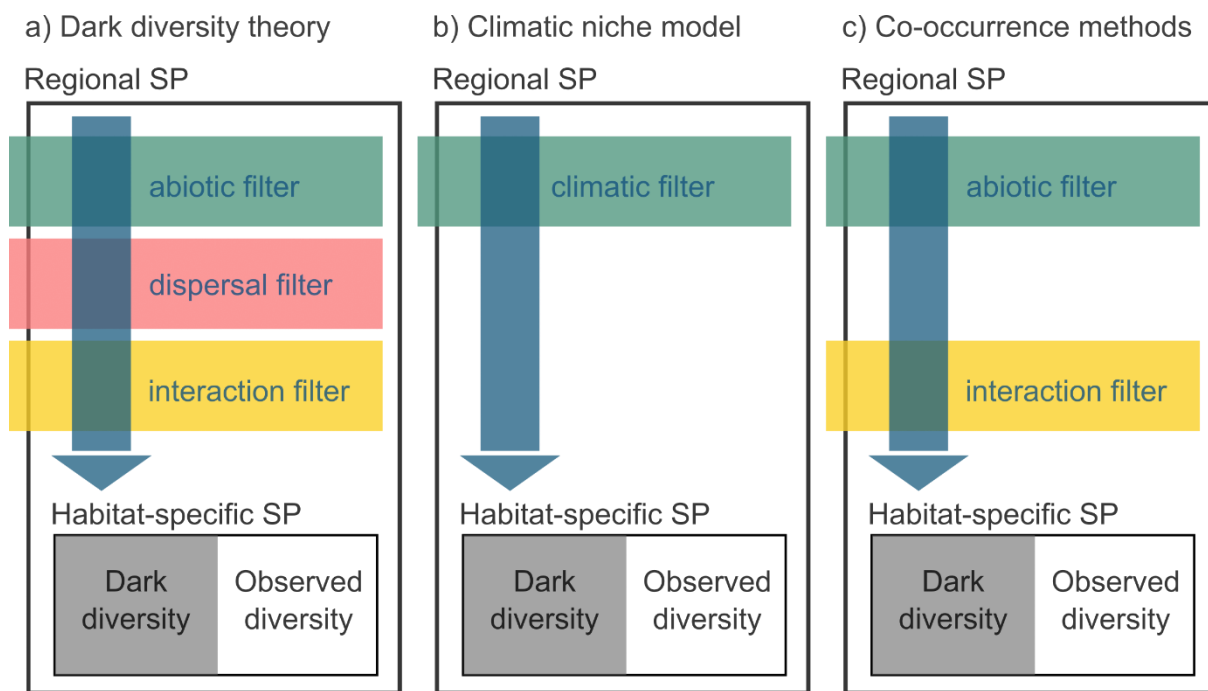
45 **Key-words:** plant ecology, Beals' index, co-occurrence-model, niche-model, method comparison, plant  
46 diversity, regional species pool, plant traits, habitat characteristics

#### 47 **Introduction**

48 Terrestrial ecosystems are increasingly affected by land-use and climate change, leading to large-scale  
49 biodiversity loss and community turnover (Theurillat & Guisan, 2001; Mooney et al., 2009; Newbold et  
50 al., 2015). Biodiversity plays an important role in ecosystem health and its loss alters ecosystem  
51 function (Hooper et al., 2012; Tilman et al., 2014). While most research has focused on the set of  
52 species that occur in an area, much less attention has gone to those species that are missing but could  
53 potentially inhabit the area (Pärtel et al., 2011). Nevertheless, to get a better understanding of  
54 community patterns and their underlying processes, such species absences hold viable additional  
55 information (Pärtel, 2014). Knowing which species from the regional species pool are absent within a  
56 given locality and identifying why, can help fine-tune conservation planning (Lewis et al., 2017). For  
57 example, if many of the absent – yet expected based on climate conditions – species are dispersal  
58 limited or cannot access the focal area due to strong dispersal barriers (i.e., habitat fragmentation),  
59 then some form of facilitated dispersal through assisted migration or actions to restore habitat  
60 connectivity is needed to restore biodiversity. However, if the nutrient conditions in the soil of the  
61 focal area are unsuitable for many of the missing species, then only providing assisted migration  
62 towards climatically suitable locations or restoring suitable climatic corridors would not be sufficient  
63 as restoration measures.

64 Species belonging to the missing part of the environmentally filtered regional species pool are defined  
65 as the so-called “dark diversity” (see Figure 1a), a concept introduced by Pärtel et al. (2011). To be part  
66 of the dark diversity, the absent species must have a reasonable probability of dispersing to and  
67 establishing viable populations in the area (i.e., by belonging to the regional species pool) and its  
68 ecological requirements (depending on the methodology used that may incorporate either only its  
69 climatic or all environmental requirements) must match the local conditions (Pärtel, 2014). As a result,  
70 species that are present in the regional surroundings of the focal locality can be locally missing because  
71 they have a lower competitive ability, are dispersal limited, are ill-adapted to abiotic conditions, or due  
72 to stochastic processes (Keddy, 1992; Riibak et al., 2015). Understanding how extrinsic abiotic  
73 conditions and intrinsic species characteristics related to competition and dispersal abilities influence  
74 a species' absence can consequently give a better view of the community assembly (Belinchón et al.,  
75 2020).

76 The dark diversity concept does not encompass the total regional species pool across different habitats  
77 but focuses on the environmentally filtered, or habitat-specific, regional species pool (Lewis et al.,  
78 2017). Combining this habitat-specific regional species pool with the local observed species  
79 composition can result in an estimate of the dark diversity (Figure 1). However, there are several  
80 methods that use different biotic and abiotic filters to estimate the habitat-specific species pool (Figure  
81 1). Depending on the method, different outcomes can be expected, as explained below. One of the  
82 main benefits of the dark diversity concept is that it enables us to compare biodiversity across various  
83 habitats or ecosystems despite significant differences in local diversity by deriving a relativized  
84 biodiversity index from the dark diversity, known as community completeness (Pärtel et al., 2011;  
85 Pärtel et al., 2013).



86

87 *Figure 1: Schematic overview of three approaches used to estimate the habitat-specific species pool (SP). a) the theoretical*  
 88 *concept of dark diversity, where the dark diversity is the non-observed set of species in a certain location, after filtering the*  
 89 *regional species pool based on abiotic, dispersal and biotic interaction limitations. In b), dark diversity is calculated using*  
 90 *climatic filtering of the regional species pool (e.g. using climatic niche models to estimate which species could occur at a*  
 91 *certain location), while c) represents commonly used co-occurrence-based methods, which integrate both abiotic and*  
 92 *interaction filters. Figure adjusted from Stephenson (2016). The combination of dark- and observed diversity encompasses the*  
 93 *habitat-specific species pool. Note that for both the methods in b) and c), several other methodological decisions can still be*  
 94 *made that might affect the outcome.*

95 Estimating dark diversity is not straightforward but can be done in multiple ways (Lewis et al., 2016,  
 96 Figure 1). The difficulty lies in estimating the habitat-specific species pool, which is, as explained above,  
 97 the set of species in a region that can persist in the environmental conditions of the target site (Pärtel  
 98 et al., 2011). It encompasses both the observed and dark diversity of the focal habitat. One could  
 99 perform extensive sampling of habitat types in a region to estimate the habitat-specific species pool  
 100 of each habitat type but this can be costly and time-consuming (de Bello et al., 2016). Therefore,  
 101 computational approaches are often implemented. Most commonly, two types of methods are used  
 102 to estimate the habitat-specific species pool, either (1) based on the abiotic niche of the species (e.g.,  
 103 using ecological indicator values or species distribution models) or (2) based on metrics of species'  
 104 co-occurrence (e.g., the Beals' probability index or the hypergeometric method) (Lenoir et al., 2010; de  
 105 Bello et al., 2016; Carmona and Pärtel, 2020).

106 Ecological indicator values are a proxy for species' ecological requirements and are often used to  
 107 characterize environmental conditions. The approach allows to identify species from the regional  
 108 species pool along environmental gradients based on their ecological preferences (Ellenberg et al.,  
 109 1991). A downside of this method is the difficulty of defining the realized niche of species since such  
 110 indicator values are rough estimates of the niche optimum along a few specific ecological gradients,  
 111 often based on expert knowledge (Lewis et al., 2016). Potentially more accurate approaches based on  
 112 abiotic conditions make use of habitat suitability models to estimate species' environmental niches  
 113 (Guisan & Thuiller, 2005). These models can be used to determine the environmental conditions  
 114 suitable for a species (Parolo et al., 2008). In this method, the accuracy of the models highly depends  
 115 on the resolution as well as on the selected set of environmental data (de Bello et al., 2016).  
 116 Additionally, predicting a species' habitat suitability based only on occurrence observations and

117 environmental data may prove to be difficult since processes like competition can play a crucial role,  
118 especially at the local scale (Cadotte & Tucker, 2017).

119 In both the above-mentioned methods, the aim is to estimate the suitability of a location based only  
120 on the environmental niche of the species, regardless of the other species co-occurring in said location.  
121 By contrast, one could also estimate the potential of finding a species at a certain location based on  
122 the presence of its associated species. The Beals' probability index can be used to calculate species co-  
123 occurrence patterns (Beals, 1984). It relies on the idea that the presence of a species that is frequently  
124 found together with another species could indicate shared suitable abiotic conditions (Ewald, 2002). If  
125 the associated species of a target species are observed, but the target species itself is not, it is part of  
126 the dark diversity. The hypergeometric method works similarly by verifying if certain species  
127 associations occur more often than predicted by chance and by estimating the dark diversity of a given  
128 species at a location from the likelihood of its co-occurrence with species present at that location  
129 (Carmona & Pärtel, 2020). The major difference between the Beals' probability index and  
130 hypergeometric method is that the hypergeometric method compares the actual number of co-  
131 occurrences between two species to the association of random pairs of species (i.e. under the  
132 assumption that there is no association). The difference between the observed and random  
133 association provides the index value, whereas for the Beals' index, the index value is only based on the  
134 observed patterns of co-occurrence (Carmona & Pärtel, 2020; Trindade et al., 2023). The advantage of  
135 these two co-occurrence-based approaches is that one only requires species composition data in the  
136 community without the need for environmental conditions. However, the prediction of the probability  
137 of a given species to belong to the dark diversity is dependent on the distribution of other species,  
138 which is especially challenging for species that are not strongly confined to particular communities or  
139 for environments where traditional communities and thus species associations are truncated (e.g., due  
140 to habitat disturbances).

141 All these methods share a common purpose: they help recognize species that belong to the habitat-  
142 specific species pool. The species not recorded in the observed diversity, but belonging to the habitat-  
143 specific species pool of the focal site are part of the dark diversity (Figure 1; Pärtel et al., 2011).  
144 Considering the absence of a standard method for calculating the habitat-specific species pool and, by  
145 extension, the dark diversity, we used both niche- and co-occurrence-based approaches. Our aim was  
146 to estimate the dark diversity around Abisko, Sweden. We wanted to explore whether these different  
147 methods would yield varying estimates of dark diversity due to their inherent filters (Figure 1). We  
148 then further explored the drivers behind the spatial patterns of this dark diversity and assessed the  
149 impact of the different methods on these drivers. The concept of dark diversity is still in its infancy and  
150 therefore only a handful of studies have explored why species are part of the dark diversity, none of  
151 which were to our knowledge conducted in subarctic environments (Belinchón et al., 2020; Moeslund  
152 et al., 2017; Riibak et al., 2015). In this study, we wanted to unravel the drivers behind (1) why some  
153 locations are missing relatively more suitable species than others, and (2) why certain vascular plants  
154 of the Scandinavian mountains are more often absent from suitable locations than others.

155 In light of the first research question, we expected locations with a higher relative dark diversity,  
156 hereafter referred to as plot-level dark diversity (i.e., a higher percentage of missing species from the  
157 habitat-specific species pool) to: (1) appear at lower elevations, as more intense competition will  
158 exclude a higher proportion of species (Jones & Gilbert, 2016); (2) be at the extreme ends of  
159 disturbance gradients, based on the intermediate disturbance hypothesis (Lembrechts et al., 2014;  
160 Rashid et al., 2021); (3) be at the extreme end of low pH and/or moisture gradients, since such  
161 conditions can be tolerated by a few species only (Gough et al., 2000; Vonlanthen et al., 2006); or (4)  
162 have low observed species richness, as these locations will be dominated by highly competitive species

163 preventing specialist species from co-occurring (Pellissier et al., 2010). Of course, these factors would  
164 act in addition to the stochasticity that always explains part of the variation in species occurrences at  
165 small spatial scales (Mohd et al., 2016).

166 The composition of dark diversity can be influenced by not only plot characteristics but also species  
167 traits. Certain traits might make some species more likely to be absent from plots, thereby contributing  
168 to the dark diversity (Moeslund et al., 2017). Therefore, we have selected six species traits related to  
169 resource-use efficiency and dispersal as these can play a key factor in plant recruitment and  
170 persistence. We predict that plant species with a higher dark diversity probability, hereafter referred  
171 to as species-level dark diversity (i.e., absent in a higher percentage of plots where they were predicted  
172 to occur) to: (1) have a higher specific leaf area (SLA), since the soils in the alpine habitats of the study  
173 area are nutrient-poor (Westoby, 1998); (2) have a lower maximum vegetative plant height, as smaller  
174 plants would be more easily outcompeted in plots were they could theoretically occur; (3) have a  
175 higher seed mass or short-distance dispersal, since these are (loosely) correlated to a limited dispersal  
176 ability and lower seed abundance, which decreases the number of successful dispersal events (Howe  
177 & Smallwood, 1982; Ozinga et al., 2005); (4) be more recently introduced in the region, as non-native  
178 species have a more limited distribution and show possible time-lags in niche filling (Alexander et al.,  
179 2016; Crooks, 2005); or finally, (5) be associated with arbuscular mycorrhizal (AM) or ectomycorrhizal  
180 (EcM) fungi, as the native vegetation in the region is dominated by ericoid mycorrhizal (ErM) species  
181 (Finlay, 2008; Tedersoo, 2017).

## 182 **2 Materials and methods**

### 183 **2.1 Study area**

184 The field data collection was performed in July and August 2021 in the Abisko area, northern Sweden  
185 (68°21'N, 18°49'E). The region has a subarctic montane climate with an average annual temperature  
186 of -0.6°C (1913-2020, although average annual temperatures have not dropped below 0°C since 2011)  
187 and average annual precipitation of 310 mm (Abisko Scientific Research Station, 400 m above sea level  
188 (a.s.l.); <https://polar.se/>). The soil is comprised of till, colluvium, and glacio-fluvial deposits (Callaghan  
189 et al., 2013). At high elevations, the area is covered in snow for about 27 weeks of the year (Callaghan  
190 et al., 2013). At low elevations, the vegetation is dominated by open birch forests (*Betula pubescens*  
191 Ehrh.), with additional presence of rowan (*Sorbus aucuparia* L.) and several willow species (*Salix* sp.).  
192 The understory vegetation often consists of heath species (e.g., dwarf birch (*Betula nana* L.), European  
193 blueberry (*Vaccinium myrtillus* L.) and black crowberry (*Empetrum nigrum* L.)), or meadow species  
194 (e.g., Alpine bistort (*Bistorta vivipara* L.), globeflower (*Trollius europaeus* L.) and Alpine saw-wort  
195 (*Saussurea alpina* DC.)) (Sonesson & Lundberg, 1974). Above the treeline (520 m a.s.l), the vegetation  
196 is dominated by alpine/arctic heathland species (e.g., blue heath (*Phyllodoce caerulea* L.), bog  
197 blueberry (*Vaccinium uliginosum* L.) and lingonberry (*Vaccinium vitis-idaea* L.)) (Kullman, 2015).

### 198 **2.2 Field data collection**

#### 199 **2.2.1 Study sites**

200 A total of 107 plots were surveyed in the vicinity of four mountain trails: Björkliden, Låktatjåkka, Nuolja,  
201 and Rallarvägen (Figure 2).



202  
 203 *Figure 2: Map of the study area around Abisko, Sweden (grey dot on the inset), with 107 surveyed plots*  
 204 *along the four hiking trails (colors) and the different survey methods (symbols).*

205 Data from new and ongoing vegetation surveys were combined, with two different methodologies: 73  
 206 1 m × 1 m plots from a long-term vegetation composition monitoring project in the area (hereafter  
 207 called ‘small plots’), as well as 34 large (10 m × 10 m) plots established in the framework of the global  
 208 DarkDivNet network (Pärtel et al., 2019). Of the 107 plots, 40 were situated along trails close to  
 209 Björkliden and around Låktatjåkka (Wedegärtner et al., 2022), 57 in the Abisko National Park on Mount  
 210 Nuolja (MacDougall et al., 2021), and 10 along the Rallarvägen.

### 211 2.2.2 Large plots

212 The vegetation monitoring method used in the large plots was based on the DarkDivNet protocol  
 213 (Pärtel et al., 2019). The plots (10 m × 10 m) were placed at a 10 m perpendicular distance from the  
 214 trail. In each plot, all vascular plants were recorded. Species were identified using the Fjällflora  
 215 (Mossberg & Stenberg 2008). Observations that could not be identified to the species level (e.g.,  
 216 *Alchemilla* sp.) were removed from the species list and thus also from the regional species pool.  
 217 Furthermore, following the DarkDivNet protocol, the maximum vegetative height (cm) was measured  
 218 with a ruler for the tallest individual of each species in all plots.

219 In every plot, we visually estimated the cover (%) of total vegetation, bare ground, rock, litter,  
 220 herbaceous vegetation, bryophytes, lichen, shrubs, and trees (> 200 cm). At the center of every plot,  
 221 the exact location was recorded with a hand-held GARMIN GPSMAP® 66i GPS receiver. Soil samples  
 222 were collected using the protocol explained below (see 2.3).

### 223 2.2.3 Small plots

224 The small plots were surveyed using the pin-point or point intercept method, which is often used to  
225 assess plant cover (Jonasson, 1988). A 1 m × 1 m plot was placed at 10 m from the trail. In one plot,  
226 100 pins were vertically dropped in 10 cm increments from left to right and top to bottom. With every  
227 pin-drop, we recorded the vascular plant species touching the pin, multiple recordings for the same  
228 species occurred when more than one individual of that species touched the pin. When the pin  
229 touched only the ground, the observation was categorized as either litter, bryophytes, bare soil, or  
230 lichen, a single hit was noted. Soil samples were collected using the same protocol as explained below  
231 (see 2.3).

## 232 **2.3 Soil sample analysis**

233 Soil samples were collected in 50 out of the 107 plots (both large and small plots). During sampling,  
234 the litter covering the soil was removed and a minimum of 300 g of soil was taken from the top 10 cm  
235 of the ground. Soil samples could not be collected along the Nuolja trail (57/107 plots) as this trail is in  
236 the Abisko National Park and no sampling permission was obtained in the year of the survey. However,  
237 50 of these plots were long-term permanent plots for which soil pH measurements were available from  
238 previous soil sampling campaigns conducted in 2018 (using the same sampling and analysis  
239 procedure). The seven remaining plots were in very close (<10 m) proximity to small plots for which  
240 pH was measured in 2018, and we therefore used the mean pH of those plots. Ultimately, pH could be  
241 obtained for all but one plot, assuming that when largely undisturbed – as was the case in the system  
242 – pH-values would only change slightly over time.

243 All soil samples were stored in a fridge at 4°C until they were analyzed between September and  
244 December 2021 at the University of Antwerp, Belgium. To measure soil pH, 25 mL of a KCl solution was  
245 added to 10 g (9.9-10.1 g) of soil. The samples were put in a shaker for an hour and afterward rested  
246 for another 60 min. Then, soil pH was measured with a 914 pH/Conductometer by Metrohm© in the  
247 liquid layer at the top of the sample after shortly manually shaking the tubes.

## 248 **2.4 Online data collection**

### 249 **2.4.1 Gridded data products**

250 To create the climatic niche models, we collected gridded climate data with a resolution of 30  
251 arcseconds (c. 1 km at the equator) for annual mean air temperature, annual precipitation, mean  
252 maximum air temperature of the warmest month, and mean minimum air temperature of the coldest  
253 month. Gridded data were downloaded from CHELSA version 1.2, representing the long-term (1979-  
254 2013) climatic conditions (Karger et al., 2017).

255 Soil temperature estimates (i.e., annual mean soil temperature, mean soil minimum temperature of  
256 the coldest month and mean soil maximum temperature of the warmest month) were obtained from  
257 the SoilTemp global maps of soil temperature (Lembrechts et al., 2021). The SoilTemp maps were  
258 derived from CHELSA monthly air temperature maps and the offset between gridded air temperature  
259 and in-situ soil temperature measurements stored in the SoilTemp database (Lembrechts et al. 2020).  
260 The gridded data, representative of the upper soil layer (top 5 cm), had the same resolution as the  
261 CHELSA data, namely 30 arcseconds.

262 Elevation was extracted from the European Digital Elevation Model (DEM) with a resolution of 25 m,  
263 obtained from Copernicus Land Monitoring Service version 1.1 (European Union, 2021).

264 Lastly, the topographic wetness index, a topographical proxy for soil moisture, was obtained from a  
265 TWI raster layer covering Europe (Haesen et al., 2021). The TWI raster, which had a spatial resolution  
266 of 25 m, was generated using the method developed by Kopecký et al. (2021).



267 All gridded data were handled in R version 4.2.1 (R Core Team, 2021) using the raster (Hijmans et al.,  
268 2012), sp (Pebesma et al., 2005), and rgdal (Keitt et al., 2010) packages to overlay the spatial  
269 coordinates of all 107 plots and extract climatic information at the plot-level.

#### 270 **2.4.2 Type of disturbance**

271 For every plot, we assigned a type of disturbance based on its proximity to hiking trails, roads, and  
272 railroad. By visual assessment in QGIS, one of the three disturbance types (hiking trail, road or railroad)  
273 was assigned to every plot. All plots were close to hiking trails, yet whenever the railroad or a road was  
274 within 150 m of the plot, its impact was considered dominant, and the hiking trail classification thus  
275 overruled. While a continuous variable for distance to the disturbance would have allowed for more  
276 nuance, adding a separate parameter for distance to the trail, to the road and to the railroad was not  
277 possible, as all plots were at a fixed distance of 10 m from a trail, and the distance to road and railroad  
278 were too strongly correlated.

#### 279 **2.4.3 Amount of bare ground**

280 Disturbances can generate patches of bare ground that can open empty niches for new species to  
281 colonize and establish themselves (Lembrechts et al., 2014). The amount of bare ground (%), here used  
282 as a proxy of disturbance, was estimated or calculated for every plot. For the large plots, this was  
283 estimated from the percentage cover of litter and bare ground. This was calculated for the small plots  
284 by summing up all the pins that touched bare ground and litter, dividing this by the total number of  
285 pins in a plot.

#### 286 **2.4.4 Plant functional traits**

287 Average maximum vegetative plant height per species was calculated from the measurements done in  
288 the large plots.

289 The specific leaf area (SLA) for every species was retrieved from data collected in the framework of the  
290 Mountain Invasion Research Network (MIREN) in the region in 2017 (published as part of the Tundra  
291 Trait Team database (TTT); Bjorkman et al., 2018). The SLA was calculated as leaf area (cm<sup>2</sup>)/dry weight  
292 (g).

293 Average seed mass per species was obtained from the global TTT database or – if not available there -  
294 the LEDA Traitbase (Bjorkman et al., 2018; Kleyer et al., 2008).

295 The dispersal type per species was also retrieved from the LEDA Traitbase and used to categorize  
296 species according to their potential for long-distance dispersal (LDD) and short-distance dispersal (SDD)  
297 (Kleyer et al., 2008). All species were considered long-distance dispersers, hence this variable was not  
298 included in further analyses.

#### 299 **2.4.5 Nativeness Index**

300 We used a continuous rather than a binary measure of the status of a species within a region, to get a  
301 more accurate view of the history of the species. Our nativeness index (NI) used historical surveys from  
302 the Global Biodiversity Information Facility ([GBIF](#)) database. It considered the first year a species was  
303 observed (year first occurrence species) and the first year in which more than 50 species were  
304 observed in the region (year first survey). If the NI was close to 1, the species was already observed at  
305 the time of the first survey. As the value approached 0, the species was observed increasingly recently  
306 for the first time and was thus more likely to be non-native.

307 
$$NI = \frac{\sqrt{\text{year (2020)} - \text{year first occurrence species}}}{\sqrt{\text{year (2020)} - \text{year first survey (1850)}}$$

308 Square roots were used in the formula to give more weight to recent differences (e.g., a first  
309 observation in 2010 vs 2020 is considered a more substantial difference than one in 1900 vs 1910). The  
310 first occurrence and the year of the first survey were obtained using the *rgbif* package (Chamberlain  
311 et al., 2021).

312 Note that the region was poor in non-native species, and those present were mostly introduced  
313 already over a century ago (Wiegman et al. 2022). This is reflected in the high values of our nativeness  
314 index (mean = 0.98, 5% lowest = 0.88). Consequently, one should not expect strong effects of  
315 nativeness on dark diversity patterns in the northern Scandes.

#### 316 **2.4.6 Mycorrhizal associations**

317 The association of plant species with the main types of mycorrhizal fungi (AM = arbuscular mycorrhiza,  
318 EcM = ectomycorrhiza, ErM = ericoid mycorrhiza and NM = no mycorrhiza) was retrieved from the  
319 FungalRoot database (Soudzilovskaia et al., 2020).

320 More details on the online data collection can be found in Appendix S1.

### 321 **2.5 Data-analysis**

#### 322 **2.5.1 Dark diversity modeling**

323 For further analysis, only species with 10 or more occurrences, were included (n=49), as sufficient  
324 observations were needed to calibrate climatic niche models and build co-occurrence matrices. We  
325 then used the same dataset in four different approaches to estimate dark diversity. All statistical  
326 analyses were conducted in R version 4.2.1 (R Core Team, 2021).

#### 327 Climatic niche modeling

328 The presence and absence of all species in every plot was used to make climatic niche models. For  
329 every species, a generalized linear model (GLM) was calibrated, with a binomial distribution containing  
330 all climatic variables and their quadratic terms as explanatory variables (i.e., annual mean air  
331 temperature, annual precipitation, maximum air temperature of the warmest month, minimum air  
332 temperature of the coldest month, annual mean soil temperature, minimum soil temperature of the  
333 coldest month, and maximum soil temperature of the warmest month) and presence/absence (1/0) of  
334 a species per plot as the response variable. Multicollinearity was checked using the Variance Inflation  
335 Factor (VIF) from the *car* package (Fox & Weisberg, 2019) and variables that increased the VIF to 5 or  
336 more were removed. The final models contained: annual precipitation, minimum soil temperature of  
337 the coldest month, maximum soil temperature of the warmest month, and their quadratic terms. No  
338 further model selection was done as we were not interested in a model identifying the drivers of the  
339 species' climatic niche, but rather wanted to approximate their climatic niche as consistently as  
340 possible.

341 To predict the probability of a species' occurrence in a specific plot, the GLM was calibrated on all  
342 remaining plots (Lembrechts et al., 2019) and the probability was estimated for that specific plot  
343 excluded from the model calibration. This leave-one-out procedure was then repeated for all plots and  
344 all species, each time predicting the probability of occurrence of a species in a plot based on a model  
345 calibrated on its occurrence pattern in all other plots. We then calculated the relative dark diversity  
346 per plot by averaging the predicted presence of each absent species in a plot and the dark diversity

347 probability per species by averaging the predicted presence of a species across all plots where it was  
348 absent.

349 The second method to estimate the dark diversity used the same climatic niche model as above. Yet,  
350 instead of continuous probability estimates, we converted niche model predictions into  
351 presence/absence estimates. For this, we calculated species-specific thresholds for presence using the  
352 function *ecospat.max.tss* from the *ecospat* package (Broennimann et al., 2022) which chooses the  
353 threshold that maximizes values for the True Skill Statistic (TSS), which assesses the accuracy of species  
354 distribution models (Allouche et al., 2006). Based on this, we created a binary dataset where the values  
355 below the threshold got a 0 (predicted to be absent) and the values above got a 1 (predicted to be  
356 present). Afterward, we removed the values where the species was observed to be present based on  
357 the vegetation surveys. To calculate the species-level dark diversity probability, we used the formula  
358 proposed by Moeslund et al. (2017), using the number of plot-level observations and predictions:

$$359 \frac{\# \text{ times in dark diversity}}{\# \text{ times in species pool}}$$

360 To calculate the relative plot-level dark diversity:

$$361 \frac{\# \text{ species in dark diversity}}{\# \text{ species in species pool}}$$

362 The habitat-specific species pool consisted of both the observed and dark species. Note that at the  
363 species level, we are estimating the probability that a species belongs to the dark diversity (dark  
364 diversity probability), while at the plot-level, we are estimating the percentage of species from the  
365 species pool that is absent (dark diversity *per se*).

#### 366 Beals' method

367 Two co-occurrence-based methods to estimate the dark diversity were used, with the first being the  
368 Beals' index (Beals, 1984), as applied by Lewis et al. (2016). We first built a species co-occurrence  
369 matrix, then calculated the Beals' index, using the *beals* function from the *vegan* package, for each  
370 species in every plot, excluding the focal species as suggested by Oksanen et al. (2022). The thresholds  
371 used to decide whether a species was part of the regional species pool were species-specific and  
372 defined as the 5th percentile of the Beals' index value for the species (Gijbels et al., 2012). Before  
373 calculating each threshold, the lowest value of the Beals' index was determined among the plots  
374 containing occurrences of the species in question, and all plots with values below this lowest value  
375 were discarded (Moeslund et al., 2017). For each plot, the dark diversity then consisted of all species  
376 from the habitat-specific species pool, except those present (Pärtel et al., 2011). To calculate the plot-  
377 and species-level dark diversity probability the same formulae as for the species-specific threshold  
378 were used.

#### 379 Hypergeometric method

380 The second method used to estimate the dark diversity was the hypergeometric method, as proposed  
381 by Carmona & Pärtel (2020). This method avoids the binary form in which dark diversity is often  
382 defined. The co-occurrence matrix used for the Beals' method was also employed in this case. To get  
383 estimates of the dark diversity, we used the function *DarkDiv* from the *DarkDiv* package, with the  
384 argument 'method' containing 'Hypergeometric' (Carmona & Pärtel, 2020). We applied this method  
385 to all species in all plots for which we obtained a probability that the species could be present in that  
386 plot. Afterward, all values for plots where the species were observed to be present were removed and  
387 a conservative threshold of 0.9 was applied as done by Trindade et al. (2023). All values below 0.9 were

388 given a 0 since we did not expect the species to be present here. To calculate the relative plot-level  
389 dark diversity, per plot the mean was taken from the remaining values (i.e. all values larger than 0.9).  
390 The same was done for the species-level dark diversity, yet here the mean was taken per species.

### 391 **2.5.2 Drivers of relative plot-level dark diversity**

392 To investigate why certain plots had a higher relative dark diversity, we created generalized linear  
393 mixed-effects models (GLMMs) with a beta distribution and logit-link function using the *glmmTMB*  
394 package (Brooks et al., 2017). Predictions from each of the four dark diversity indices (the two  
395 approaches based on niche models, the Beals' index, and the hypergeometric approach) were used as  
396 the response variable.

397 These plot-level models contained elevation, soil pH, type of disturbance, amount of bare ground, TWI,  
398 observed species richness and plot size as explanatory variables. The plots were situated along various  
399 trails. To account for this hierarchical sampling design, the model included a random intercept for plot  
400 number nested within trail identity. Multicollinearity and distribution of residuals were checked using  
401 the Variance Inflation Factor (VIF) and the *DHARMA* package (Hartig, 2022) and deemed not violated.  
402 Due to the low sample size, we limited ourselves to linear patterns and did not include two-way  
403 interaction terms since these more complex models could not converge. For the same reason,  
404 quadratic effects were not tested, even though theoretically they could be expected for pH and soil  
405 moisture. However, within our study system both the pH and moisture gradient only reached extreme  
406 values on one side of the gradient (e.g., highly acidic yet no highly basic soils).

407 No further model selection was performed (Hartig, 2018). The variance explained by the full model  
408 was obtained using the *performance* function from the *performance* package (Lüdecke et al., 2021).  
409 To determine the proportion of explained variance of every variable, we followed a variation  
410 partitioning approach. First, the variance of the full model was calculated. Afterward, for every  
411 explanatory variable, a model was made consisting of all variables except the focal variable. By  
412 extracting the marginal  $R^2$  of the individual models from the  $R^2$  of the full model, the variance of the  
413 focal variable was obtained (Legendre & Legendre, 1998). Community completeness was also  
414 calculated for each plot and every method as  $\ln(\text{observed richness/dark diversity})$  (Pärtel et al., 2013).  
415 A linear mixed model was created using the *lmer* function from the *lme4* package (Bates et al., 2015)  
416 with plot as a random factor to compare whether the community completeness differed significantly  
417 depending on the method. The distribution of the residuals was checked using the *DHARMA* package  
418 (Hartig, 2022) and assumptions were not deemed violated. As one needs to assess community  
419 completeness using species numbers, the community completeness based on the climatic niche  
420 models had to be calculated using a species-specific threshold as well, thus resulting in the same values  
421 as in the original dark diversity assessment using climatic niche models with a threshold. We thus  
422 maintained only one of these in the comparison.

423

### 424 **2.5.3 Drivers of species-level dark diversity probability**

425 To investigate why certain species had a higher dark diversity probability, we created GLMs with a beta  
426 distribution and logit-link function using the *betareg* package (Cribari-Neto & Zeileis, 2010) with  
427 predictions from each of the used dark diversity indices (based on the niche models, the Beals' index,  
428 and the hypergeometric approach) as a response variable.

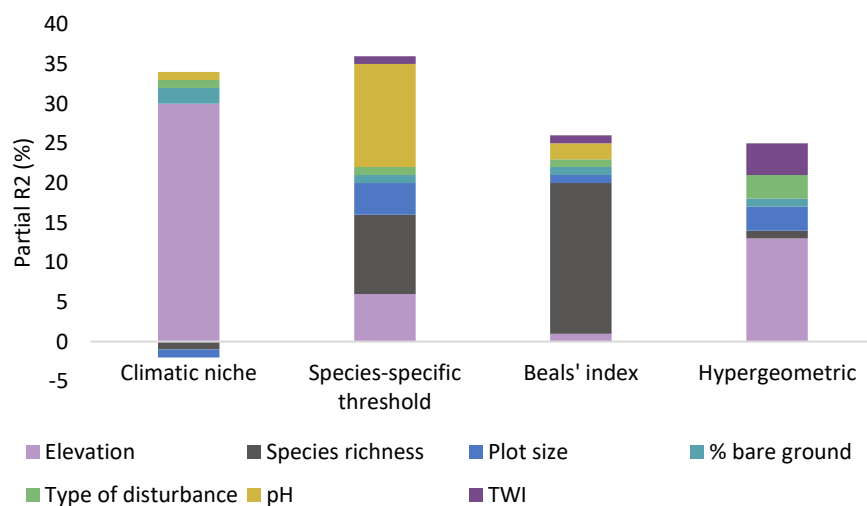
429 First, full models were made separately for each dark diversity index that contained the nativeness  
430 index, maximum vegetative plant height, specific leaf area, dispersal type, seed mass, and mycorrhizal

431 association as explanatory variables and species-level dark diversity as the response variable.  
 432 Assumptions of multicollinearity and distribution of residuals were tested and not violated. Here as  
 433 well, two-way interaction terms could not be tested and no further model selection was performed  
 434 (Hartig, 2018). Afterward, pairwise comparisons were conducted on the categorical parameters using  
 435 the *emmeans* package (Lenth, 2022).

### 436 3 Results

#### 437 3.1 Plot-level dark diversity

438 Depending on the method, we could explain between 39% and 87% of the variance in plot-level dark  
 439 diversity. In two cases (climatic niche models and hypergeometric method), elevation was responsible  
 440 for the largest share, while in the two other cases (species-specific threshold and Beals' index) species  
 441 richness was the most dominant factor (Figure 3). On average across all models, elevation explained  
 442 13%, species richness 7%, and plot size, type of disturbance, amount of bare ground, pH and TWI an  
 443 additional 2%, 1%, 2%, 4% and 2%, respectively. Note that due to the nature of the variance  
 444 partitioning calculations, variances do not necessarily add up to the total variance of the full model.



445

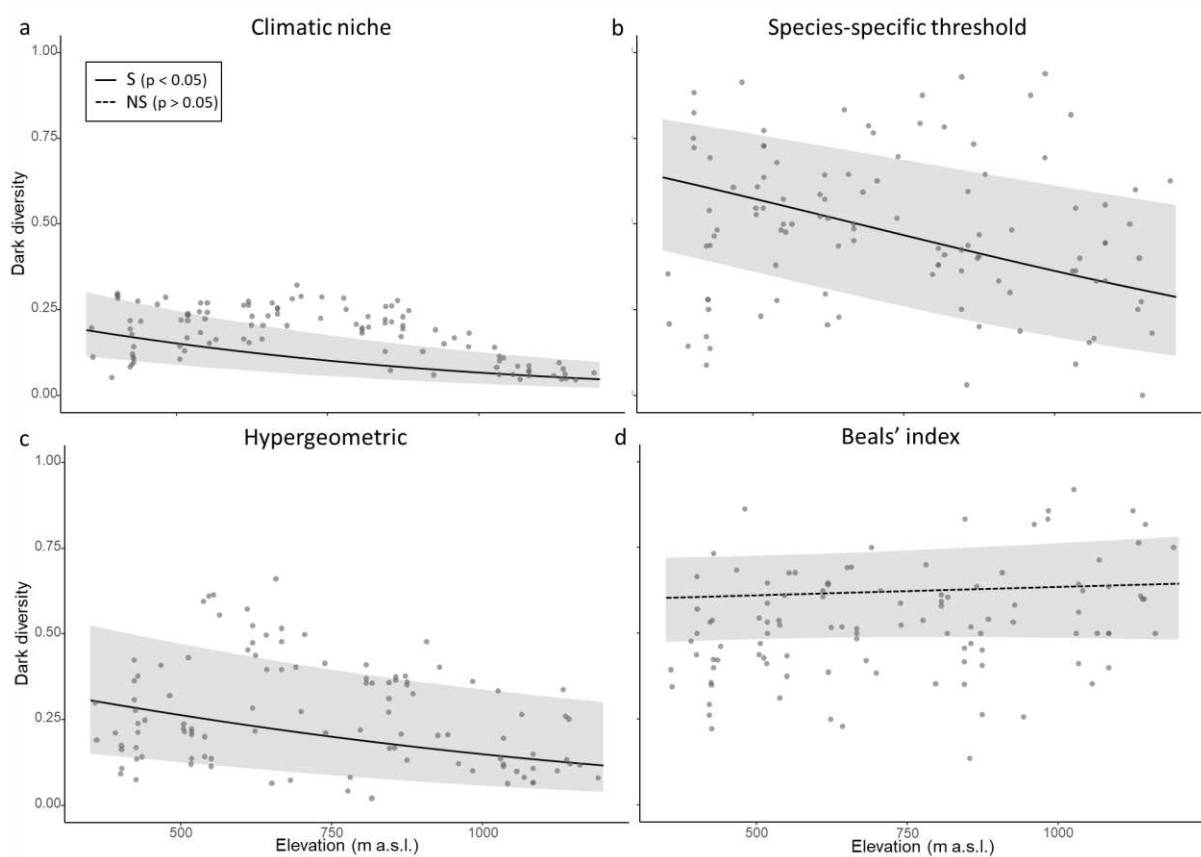
446 *Figure 3: Variance partitioning (expressed in % and calculated using the marginal R<sup>2</sup>) of the different*  
 447 *explanatory variables in the GLMMs of the plot-level analyses on the predictions of each of the four*  
 448 *different dark diversity methods. TWI = topographic wetness index.*

449 In three out of the four methods used, the plot-level dark diversity decreased significantly across the  
 450 elevation gradient (Table 1; Figure 4). Only in the model based on the Beals' index did elevation not  
 451 have a significant influence (Table 1; Figure 4d).

452 *Table 1: Models explaining the plot-level dark diversity using the different dark diversity estimation*  
 453 *methods: coefficients (p-values: \* p<0.05; \*\* p<0.01; \*\*\* p<0.001). The factor used for the intercept*  
 454 *was allocated alphabetically and all other factors were compared to this baseline. CN = climatic niche*  
 455 *models; SS = species-specific threshold; Hyper = hypergeometric method; Beals = Beals' index; Elev =*  
 456 *elevation; SR = species richness; TOD = type of disturbance; TWI = topographic wetness index.*

Model	Intercept (Road)	Elev	SR	Plot size (10m x 10m)	TOD Hiking trail	TOD Railroad	% bare ground	pH	TWI	AIC
CN	-0.327	- 0.00 1***	- 0.029** *	0.079	0.524	-0.251	-0.001*	-0.022	-0.014	-370
SS	3.00***	- 0.00 1**	- 0.105** *	-0.408*	0.281	-0.165	-0.001	- 0.262* **	0.038	-140
Hyper	0.101	- 0.00 1**	0.01	-0.304	0.416	-0.177	-0.006	-0.001	-0.071	-137
Beals	1.04*	10 <sup>-4</sup>	- 0.082** *	-0.121	-0.112	-0.345	0.001	0.032	0.001	-195

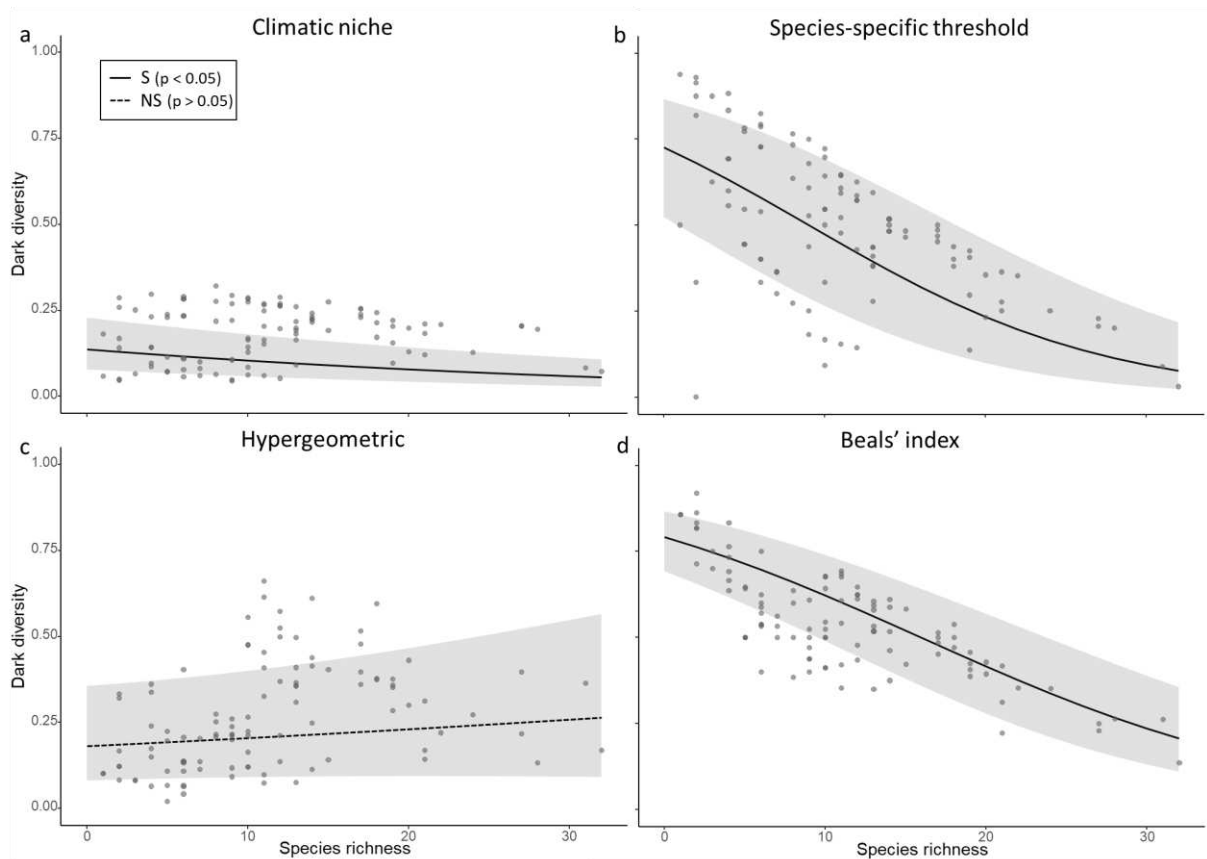
457



458  
 459 *Figure 4: Marginal effects plots of the plot-level dark diversity as a function of elevation (m a.s.l.). The*  
 460 *grey area indicates the 95% confidence interval and the grey dots are the raw data points. Dark*  
 461 *diversity was estimated using a) the climatic niche models, b) the climatic niche models followed by the*  
 462 *species-specific threshold, c) the hypergeometric method and d) the Beals' index. S = significant; NS =*  
 463 *non-significant.*

464 The plot-level dark diversity decreased significantly with increasing species richness in three cases  
 465 (Table 1; Figure 5a, 5b, 5d), yet increased with increasing species richness when using the  
 466 hypergeometric method, albeit not significantly (Table 1; Figure 5c).

467



468  
 469 *Figure 5: Marginal effects plots of the plot-level dark diversity as a function of species richness. The*  
 470 *grey area indicates the 95% confidence interval, and the grey dots are the raw data points. a) the*  
 471 *climatic niche models, b) the climatic niche models followed by the species-specific threshold, c) the*  
 472 *hypergeometric method and d) the Beals' index. S = significant; NS = non-significant.*

473 Furthermore, our results indicate that only the climatic niche model had a significant relationship  
 474 between dark diversity and bare ground. Moreover, only the climatic niche model followed by the  
 475 species-specific threshold had significant relationships with plot size and pH (Appendix S2, Figure S1a).  
 476 In the remaining two models, none of the other variables were found to be significant predictors of  
 477 dark diversity.

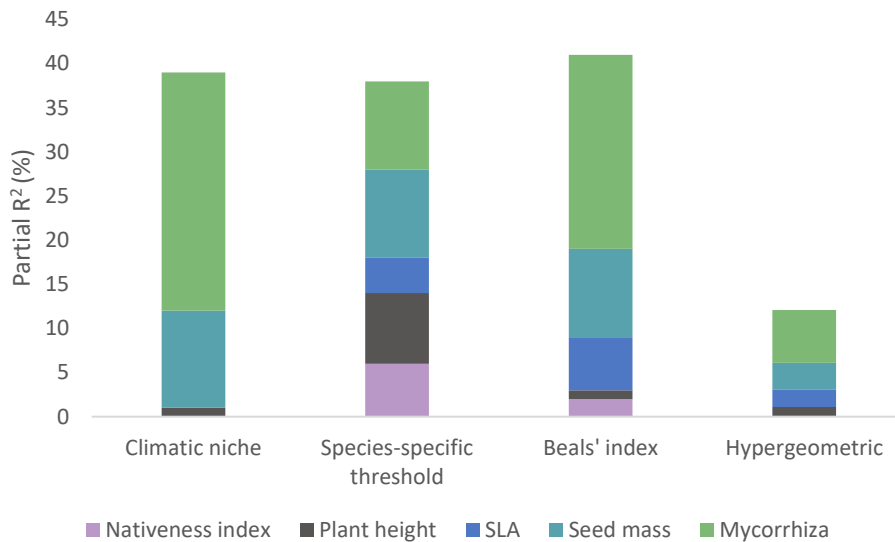
478 Lastly, the community completeness based on the Beals' index was significantly lower than the  
 479 community completeness based on the other two methods (Appendix S2, Figure S2).

### 480 **3.2 Species-level dark diversity**

481 Depending on the method, we could explain between 8% and 45% of the variance in species-level dark  
 482 diversity (Figure 6). In all cases, mycorrhizal association was responsible for the largest share (Figure  
 483 6). On average across all models, mycorrhizal association explained 16%, seed mass 9%, specific leaf  
 484 area 3% and the nativeness index and the maximum vegetative plant height an additional 2% and 3%,  
 485 respectively. Note that due to the nature of the variance partitioning calculations, variances do not  
 486 necessarily add up to the total variance of the full model.

487





488

489 *Figure 6: Variance partitioning (expressed in % and calculated using the marginal R<sup>2</sup>) of the different*  
 490 *explanatory variables in the GLMs of the species-level analyses on the predictions of each of the four*  
 491 *different dark diversity methods. SLA = specific leaf area.*

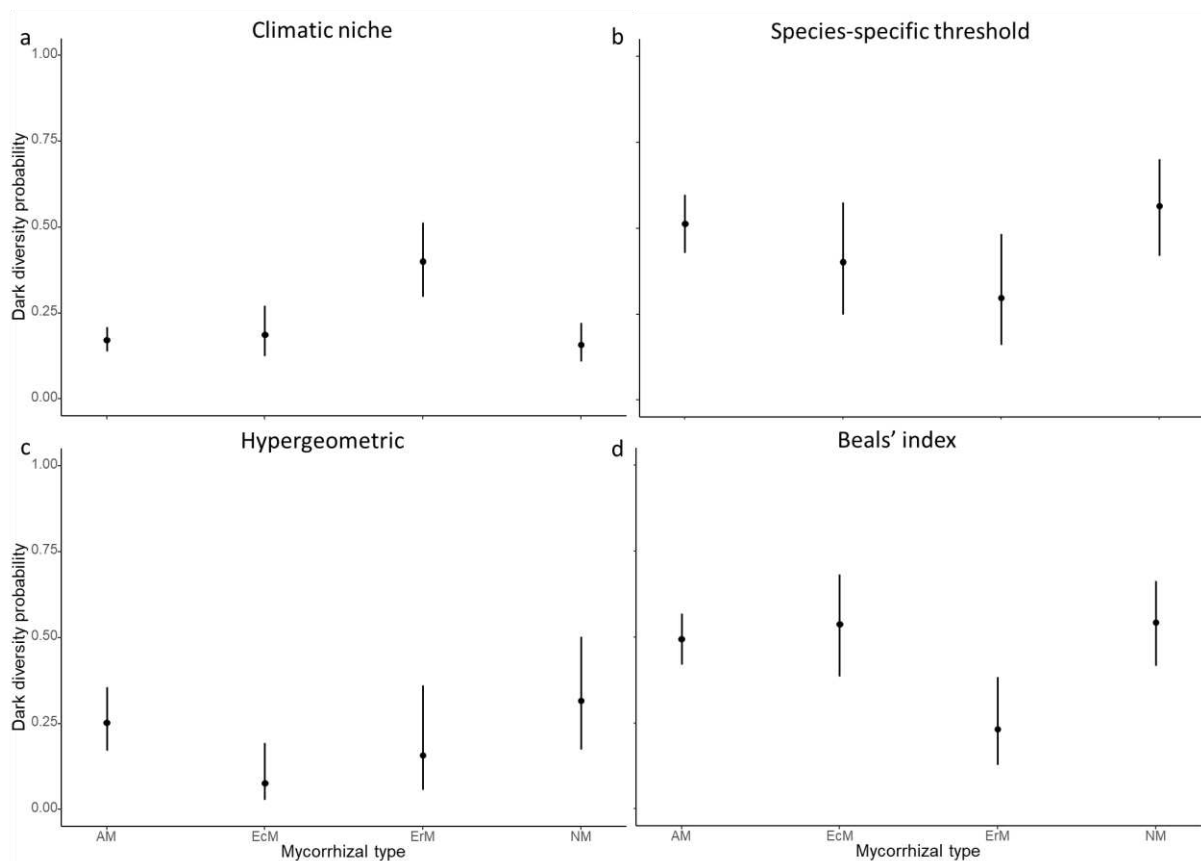
492 Mycorrhizal status was the only significant parameter in the climate niche model approach, with  
 493 ericoid mycorrhizae differing significantly from AM, EcM and NM (Figure 7; Table 2; Appendix S3).  
 494 Species with a symbiotic ericoid mycorrhizal association had a significantly higher dark diversity than  
 495 all other associations when using the climatic niche models (Table 2; Figure 8a). However, the opposite  
 496 was true when using the Beal's index and climatic niche model followed by the species-specific  
 497 threshold (Table 2; Figure 7b, d). For the Beals' index the contrast test also revealed that ericoid  
 498 mycorrhizae differed significantly from AM, EcM and NM (Figure 7d, Appendix S3). For the species-  
 499 specific threshold, the contrast test only showed a borderline significant difference between ErM and  
 500 NM (Figure 7b; Appendix S3). Lastly, and even more contrasting, species with a symbiotic  
 501 ectomycorrhizal association had a significantly lower dark diversity than all other associations when  
 502 using the hypergeometric method (Figure 7c). The contrast test also revealed that EcM differed  
 503 significantly from AM and NM (Appendix S3).

504 *Table 2: Models explaining the plot-level dark diversity using the different dark diversity estimate*  
 505 *methods: coefficients (p-values: \* p<0.05; \*\* p<0.01; \*\*\* p<0.001). The factor used for the intercept*  
 506 *was allocated alphabetically and all other factors were compared to this baseline. CN = climatic niche*  
 507 *model; SS = species-specific threshold; Hyper = hypergeometric method; Beals = Beals' index; AM =*  
 508 *arbuscular mycorrhiza; EcM = ectomycorrhiza; ErM = ericoid mycorrhiza; NM = no mycorrhiza; MVH =*  
 509 *maximum vegetative plant height; SLA = specific leaf area; NI = nativeness index; SM = seed mass.*

Model	Intercept (AM)	EcM	ErM	NM	MVH	SLA	NI	SM	AIC
CN	-0.043	0.108	1.17***	-0.101	-10 <sup>-4</sup>	-10 <sup>-4</sup>	-1.37	-0.068	-72

SS	-5.96	0.453	-0.916*	0.208	$-10^{-3}$	$-10^{-3}$	6.95	0.082	-11
Hyper	-3.66	-1.40*	-0.597	0.314	$10^{-3}$	$-10^{-3}$	3.42	0.121	-38
Beals	1.04*	0.170	-1.17***	0.193	$-10^{-4}$	-0.001	-3.28	-0.089	-19

510



511

512 *Figure 7: Prediction of the species-level dark diversity in relation to the mycorrhizal type based on the*  
513 *beta regression model. The black dots show the average dark diversity per individual factor whereas*  
514 *the error bars show the standard deviation. AM = arbuscular mycorrhiza; EcM = ectomycorrhiza; ErM*  
515 *= ericoid mycorrhiza; NM = no mycorrhiza. Dark diversity estimated using a) the climatic niche models,*  
516 *b) species-specific threshold, c) the hypergeometric method and d) the Beals' index.*

517

None of the other variables had a significant influence on the species-level dark diversity.

518

## 4. Discussion

519

### 4.1. Plot-level dark diversity

520 We found relatively consistent patterns in the drivers of dark diversity at the plot-level, but much less  
521 consistency was observed at the species level. Plot-level dark diversity was most consistently related  
522 to elevation, with plots at higher elevations having a lower plot-level dark diversity - and thus fewer  
523 expected species missing - than plots at lower elevations. This was true for both niche-based methods  
524 as well as for the hypergeometric method, yet not for the Beals' index, in which elevation was not  
525 significant. Such a decline with elevation is in line with ecological theory. Indeed, under harsh  
526 environmental conditions, competitive interactions are often replaced by mutualistic ones, or  
527 competition is at least lowered in intensity, thereby reducing the exclusion of less competitive species  
528 with a lower dark diversity as a result (Callaway et al., 2002; Klanderud, 2010; Lembrechts et al., 2018).  
529 Additionally, the presence of more ruderal and competitive species in the lowlands compared to the  
530 stress-tolerant species higher up in the mountains along roadsides also suggests that reduced  
531 competition can be one of the main drivers behind the lower dark diversity at higher elevations  
532 (Lembrechts et al., 2014). Furthermore, climatic conditions are usually milder in the lowlands, making  
533 them suitable for a broader set of species (Körner, 2021). Consequently, since more species can be  
534 present in these plots, it is also more likely that at least some of them are excluded, resulting in a  
535 higher number of species belonging to the dark diversity. As the co-occurrence-based metrics  
536 accounted for some of these factors (e.g., lower expectancy of species in plots dominated by species  
537 that traditionally outcompete them), it should come as no surprise that elevation was not significant  
538 in the model for the Beals' index.

539 Species richness was identified as a key driver of plot-level dark diversity in three out of the four  
540 methods. Its effect was negative for all but the hypergeometric method for which it was not significant,  
541 thus largely following our hypothesis. In this system, plots with a low number of species are likely to  
542 be dominated by highly competitive species, which can prevent the establishment of several species  
543 that could in theory occur there (Pellissier et al., 2010). Indeed, plots with a low species richness in the  
544 study system were often dominated by *Empetrum nigrum*. It is an efficient competitor for nutrients,  
545 can grow on soils with low pH, and has allelopathic effects against seed germination and the growth  
546 of surrounding species (Tybirk et al., 2000), and can possibly direct several species from the regional  
547 species pool locally to the dark diversity. Our results seem to support the study by Fløjgaard et al.  
548 (2020) who found that competitive species have an adverse effect on species richness, leading to an  
549 increase in dark diversity. Nevertheless, it is possible that approaches based on species co-occurrences,  
550 such as the hypergeometric method and the Beals' index, already account for this effect of  
551 competition.

552 Finally, the amount of bare ground, soil pH and plot size also appeared to have a significant effect on  
553 the plot-level dark diversity, but this was only the case for the niche-based methods. No other variables  
554 were significant for the other two methods which already indicates that these models should be  
555 handled with caution.

#### 556 **4.2 Species-level dark diversity**

557 Mycorrhizal association was the only variable with significant influence, across all methods, on the  
558 species-level dark diversity across all methods. However, while species with a symbiotic ericoid  
559 mycorrhizal association had a significantly higher dark diversity than all other associations when using  
560 the climatic niche models, the opposite was true for the climatic niche model followed by a species-  
561 specific threshold and the Beals' method. Noteworthy, when using the hypergeometric method  
562 species with a symbiotic ectomycorrhizal association had a significantly lower dark diversity than all  
563 other associations. These contrasting results highlight the differences between the different methods  
564 used to estimate dark diversity. In the Scandinavian mountains, the species with an ErM association

565 (e.g. *E. nigrum* and *V. vitis-idaea*) were virtually not climate-limited (occurring in 64 and 63 out of the  
566 107 plots, respectively) and could in theory, based on their climatic niche, be present in all plots.  
567 Therefore, their dark diversity probability ended up being very high in any plot where they were  
568 absent, simply because of the underlying modeling approach. We aimed to correct this issue by using  
569 species-specific thresholds, yet here again mycorrhizal type was withheld as significant.

570 These ErM-associated species not only dominated the studied landscape, but they were also often  
571 found in strong association with each other, resulting in clear predictions of their presence once one  
572 of them was present, when using the Beals' index. As their spatial connection in the field was so  
573 consistent, their estimated dark diversity using these methods ended up relatively low. Additionally,  
574 as ErM-fungi are the most dominant and widespread fungi in tundra regions (Tendersoo, 2017), in  
575 theory, there ought to be enough coverage of ErM-fungi so that the establishment of species  
576 associated with them should not be hampered. Consequently, there should be less reason for the  
577 species to be absent in areas where they could potentially occur than for AM-associated species  
578 (Tendersoo, 2017). All of this suggests that the observed higher dark diversity estimates for ErM-  
579 associated species based on the climatic niche approach are most likely a methodological artefact.  
580 These methodological issues could also explain why such little consistency was observed for the other  
581 studied drivers of species-level dark diversity, calling for caution when interpreting findings from any  
582 such dark diversity estimate separately.

### 583 **4.3 Comparison of methods and uncertainties**

584 In this paper, we estimated dark diversity using both niche-based and co-occurrence-based methods,  
585 which are often used interchangeably in the scientific literature. However, our results suggest that  
586 both approaches have significantly different assumptions and, as a result, get relatively incomparable  
587 results. Indeed, the niche-based approaches estimate the dark diversity as the set of species that could  
588 occur at a certain location based on their climatic niche or other environmental filters. The latter  
589 drivers are then often used as explanatory variables for the observed dark diversity, as done in the  
590 underlying study. For example, reduced competitive interactions in sites with larger percentages of  
591 bare ground would result in lower dark diversity, as is hinted at by our results.

592 Co-occurrence-based methods, on the other hand, estimate dark diversity simply from the neighboring  
593 species with which a target species is usually associated. These approaches incorporate biotic  
594 interactions inherently in the dark diversity estimate. However, they do exclude species from the dark  
595 diversity for which the climatic conditions fall within their climatic limits, yet whose co-occurring  
596 species are also missing at a site. The latter could be especially problematic in diverse communities  
597 with high beta diversity, or areas with truncated, reduced, or novel communities as a result of  
598 anthropogenic land use or climatic changes (Christensen et al., 2021).

599 Perhaps more worryingly, within each type of dark diversity estimation method, results were not  
600 necessarily in agreement with each other. We found largely different findings, especially for species-  
601 level dark diversity, when using climatic niches with or without species-specific thresholds, as well as  
602 when using the hypergeometric method versus the Beals' index. Additionally, the community  
603 completeness also differed significantly, depending on the method used. As such, our results highlight  
604 the need for caution and transparency when calculating and interpreting dark diversity estimates, as  
605 the conclusions depend heavily on the methodological decisions one makes, and methods should thus  
606 be tailored to the specific research questions.

607 Of course, several alternative methods could still be used to estimate dark diversity, and many  
608 adjustments to the methods used above could be proposed. For example, one could use global  
609 datasets such as GBIF to model the climatic niche, rather than data from the study region only. Using  
610 global datasets for such broader-scale niche models could result in a more accurate estimate of the  
611 climatic niche since the entire climatic niche could be modelled, rather than a truncated version as  
612 results from regional data (Bazzichetto et al., 2023). However, most of these global datasets lack  
613 absence data and presences are obtained using a wide variety of methodologies and spatial resolutions  
614 (Tessarolo et al., 2014), while abiotic data is at the global scale often only available at coarser resolution  
615 (Lembrechts et al., 2019). This could also make the predictions less accurate. Additionally, there is the  
616 possibility of mismatches, especially for rare species, since global datasets can be spatially biased  
617 (Meyer et al., 2016). Therefore, predicting local climatic niches based on global data can make it more  
618 difficult to figure out whether the absences are due to a bias in the global dataset or the drivers under  
619 investigation. Furthermore, it is worth mentioning that alternative thresholds could be used for the  
620 species-specific method, such as Cohen's Kappa or Area Under the Curve (AUC). The chosen TSS  
621 threshold in this study may be affected by the low prevalence of species (Leroy et al., 2018). However,  
622 since we only used the relatively common species, the issue of low prevalence should not pose a  
623 notable concern (Allouche et al., 2006; Wunderlich et al., 2019). These alternative threshold methods  
624 were not examined in this particular study as this may further complicate methodological decisions for  
625 dark diversity estimation. Hence, we suggest that more research is needed to investigate the impact  
626 of alternative thresholds when using species-specific methods.

627 The most promising avenue could perhaps come from an approach that combines both climatic niches  
628 with co-occurrences, such as joint Species Distribution Models (jSDMs; Pollock et al., 2014). This recent  
629 class of distribution models draws information from species co-occurrences and explains spatial  
630 variation in species distributions by extending standard species distribution models with species–  
631 species associations. Such an approach could potentially allow distinguishing through one model  
632 between absences driven by environmental unsuitability, biotic interactions, or other drivers.  
633 Nevertheless, Carmona & Pärtel (2020) did find that jSDMs could not outperform the hypergeometric  
634 method, yet they do substantially increase computational time.

#### 635 **4.5 Conclusions**

636 The concept of dark diversity is still in its infancy, yet its contribution to understanding community  
637 completeness and its use in nature conservation has already been shown to be significant (Lewis et al.,  
638 2017; Riibak et al., 2015). In this context, it is crucial to determine whether a species' absence is a  
639 result of species-specific traits or plot characteristics, be it abiotic factors or biotic interactions, which  
640 is something traditional biodiversity studies that only focus on species presences cannot provide. We  
641 here compared different methodological approaches to estimate dark diversity and showed significant  
642 divergence in predicted drivers of dark diversity based on the method used, calling for caution when  
643 interpreting statistical findings on dark diversity estimates. Given the high level of variation in outcome  
644 between methods, it is currently not possible to recommend one or the other. More comparative  
645 studies in different environments are thus necessary to elaborate further on the search for a robust  
646 methodology to estimate dark diversity. Nevertheless, we can generally conclude that areas at low  
647 elevations, and, to a certain extent, with a low species richness showed a higher plot-level dark  
648 diversity, largely due to natural processes such as competitive dominance. How valid these findings  
649 are for patterns in dark diversity in other (mountain) areas across the globe remains to be seen, yet  
650 the significant effect of methodological decisions on conclusions should remind us that any other  
651 regional study on dark diversity should be cautious in its conclusions. Nonetheless, one could assume

652 that dark diversity will indeed decrease with increasing elevation since only more specialized species  
653 can survive at higher elevations, and competition is lower.

#### 654 **Acknowledgments**

655 We thank the master students Renée Lejeune and Jasmine Spreewers for their assistance in gathering  
656 data during the summer of 2021. Additionally, we extend our appreciation to Stef Haesen for supplying  
657 us with the raster layer for the topographic wetness index (TWI).

#### 658 **Author contribution**

659 J.J.L. and L.H. conceived the research idea; L.H., D.W. and J.C. collected data; L.H. performed statistical  
660 analyses with guidance from J.J.L.; L.H. and J.J.L. wrote the paper with contributions from K.V.M.; all  
661 authors discussed the results and commented on the manuscript.

#### 662 **Data availability statement**

663 All data and codes that support the findings of this study are available on Zenodo  
664 <https://zenodo.org/record/8059877>.

#### 665 **References**

- 666 Alexander, J. M., Lembrechts, J. J., Cavieres, L. A., Daehler, C., Haider, S., Kueffer, C. et al., (2016)  
667 Plant invasions into mountains and alpine ecosystems: current status and future challenges.  
668 *Alpine Botany*, 126, 89–103. <https://doi.org/10.1007/s00035-016-0172-8>
- 669 Allouche, O., Tsoar, A., & Kadmon, R. (2006) Assessing the accuracy of species distribution models:  
670 prevalence, kappa and the true skill statistic (TSS). *Journal of applied ecology*, 43, 1223–1232.  
671 <https://doi.org/10.1111/j.1365-2664.2006.01214.x>
- 672 Auerbach, N. A., Walker, M. D., & Walker, D. A. (1997) Effects of roadside disturbance on substrate  
673 and vegetation properties in arctic tundra. *Ecological Applications*, 7, 218–235.  
674 [https://doi.org/10.1890/1051-0761\(1997\)007\[0218:EORDOS\]2.0.CO;2](https://doi.org/10.1890/1051-0761(1997)007[0218:EORDOS]2.0.CO;2)
- 675 Bazzichetto, M., Lenoir, J., Da Re, D., Tordoni, E., Rocchini, D., Malavasi, M. et al. (2023) Sampling  
676 strategy matters to accurately estimate response curves' parameters in species distribution  
677 models. *Global Ecology and Biogeography*. <https://doi.org/10.1111/geb.13725>
- 678 Beals, E. W. (1984) Bray-curtis ordination: An effective strategy for analysis of multivariate ecological  
679 data. *Advances in Ecological Research*, 14, 1–55. <https://doi.org/10.1111/oik.07308>
- 680 Belinchón, R., Hemrová, L., & Münzbergová, Z. (2020) Functional traits determine why species belong  
681 to the dark diversity in a dry grassland fragmented landscape. *Oikos*, 129, 1468–1480.  
682 <https://doi.org/10.1111/oik.07308>
- 683 Bjorkman, A. D., Myers-Smith, I. H., Elmendorf, S. C., Normand, S., Thomas, H. J. D., Alatalo, J. M. et al.  
684 (2018) Tundra Trait Team: A database of plant traits spanning the tundra biome. *Global  
685 Ecology and Biogeography*, 27, 1402–1411. <https://doi.org/10.1111/geb.12821>
- 686 Broennimann, O., Di Cola, V., Guisan, A. (2022). *Ecospat: spatial ecology miscellaneous methods.  
687 Version 3.4*. Available at <https://CRAN.R-project.org/package=ecospat> [Accessed 16 March  
688 2022]
- 689 Brooks, M. E., Kristensen, K., van Benthem, K. J., Magnusson, A., Berg, C. W., Nielsen, A. et al.  
690 (2017) “glmmTMB Balances Speed and Flexibility Among Packages for Zero-inflated  
691 Generalized Linear Mixed Modeling.” *The R Journal*, 9, 378–400.
- 692 Cadotte, M. W., Tucker, C. M. (2017) Should environmental filtering be abandoned? *Trends in ecology*

693 *and evolution*, 32, 429–437. <https://doi.org/10.1016/j.tree.2017.03.004>

694 Callaghan, T. V., Jonasson, C., Thierfelder, T., Yang, Z., Hedenås, H., Johansson, M. et al. (2013)

695 Ecosystem change and stability over multiple decades in the Swedish subarctic: Complex

696 processes and multiple drivers. *Philosophical Transactions of the Royal Society B: Biological*

697 *Sciences*, 368, 1–17. <https://doi.org/10.1098/rstb.2012.0488>

698 Callaway, R. M., Brooker, R. W., Choler, P., Kikvidze, Z., Lortie, C. J., Michalet, R. et al. (2002) Positive

699 interactions among alpine plants increase with stress. *Nature*, 417, 844–848.

700 <https://doi.org/10.1038/nature00812>

701 Carmona, C. P., & Pärtel, M. (2020) Estimating probabilistic site-specific species pools and dark

702 diversity from co-occurrence data. *Global Ecology and Biogeography*, 30, 316–326.

703 <https://doi.org/10.1111/geb.13203>

704 Chamberlain, S., Barve, V., Mcglinn, D., Oldoni, D., Desmet, P., Geffert, L., & Ram, K. (2021) *rgbif:*

705 *Interface to the Global Biodiversity Information Facility API. Version 3.6.0.* Available at

706 <https://CRAN.R-project.org/package=rgbif> [Accessed 15 May 2021]

707 Christensen, E., Christensen, B., & Christensen, S. (2021) Problems in using Beals' index to detect

708 species trends in incomplete floristic monitoring data (Reply to Bruelheide et al. (2020)).

709 *Diversity and Distributions*, 27, 1324–1327. <https://doi.org/10.1111/ddi.13276>

710 Cribari-Neto, F., Zeileis, A. (2010) Beta Regression in R. *Journal of Statistical Software*, 34, 1–24.

711 Crooks, J. A. (2005) Lag times and exotic species: The ecology and management of biological invasions

712 in slow-motion. *Ecoscience*, 12, 316–329. <https://doi.org/10.2980/i1195-6860-12-3-316.1>

713 de Bello, F., Fibich, P., Zelený, D., Kopecký, M., Mudrák, O., Chytrý, M. Et al. (2016) Measuring size and

714 composition of species pools: a comparison of dark diversity estimates. *Ecology and Evolution*,

715 6, 4088–4101. <https://doi.org/10.1002/ece3.2169>

716 Ellenberg, H., Weber, H.E., Düll, R., Wirth, V., Werner, W. & Paulißen, D. (1991) *Zeigerwerte von*

717 *Pflanzen in Mitteleuropa*. Scripta Geobotanica. European Union, Copernicus Land Monitoring Service

718 2021, European Environment Agency (EEA).

719 Ewald, J. (2002) A probabilistic approach to estimating species pools from large compositional

720 matrices. *Journal of Vegetation Science*, 13, 191–198. [https://doi.org/10.1111/j.1654-](https://doi.org/10.1111/j.1654-1103.2002.tb02039.x)

721 [1103.2002.tb02039.x](https://doi.org/10.1111/j.1654-1103.2002.tb02039.x)

722 Finlay, R. D. (2008) Ecological aspects of mycorrhizal symbiosis: With special emphasis on the

723 functional diversity of interactions involving the extraradical mycelium. *Journal of*

724 *Experimental Botany*, 59, 1115–1126. <https://doi.org/10.1093/jxb/ern059>

725 Fløjgaard, C., Valdez, J. W., Dalby, L., Moeslund, J. E., Clausen, K. K., Ejrnæs, R. et al. (2020) Dark

726 diversity reveals importance of biotic resources and competition for plant diversity across

727 habitats. *Ecology and Evolution*, 10, 6078–6088. <https://doi.org/10.1002/ece3.6351>

728 Fox, J., & Weisberg, S. (2011). *An R companion to applied regression* (2nd edition). SAGE Publications

729 Inc.

730 Gijbels, P., Adriaens, D. & Honnay, O. (2012) An orchid colonization credit in restored calcareous

731 grasslands. *Ecoscience*, 19, 21–28. <https://doi.org/10.2980/19-1-3460>

732 Gough, L., Shaver, G. R., Carroll, J., Royer, D. L., & Laundre, J. A. (2000) Vascular plant species richness

733 in Alaskan arctic tundra: The importance of soil pH. *Journal of Ecology*, 88, 54–66.

734 <https://doi.org/10.1046/j.1365-2745.2000.00426.x>

735 Grieve, I. C. (2000) Effects of human disturbance and cryoturbation on soil iron and organic matter

736 distributions and on carbon storage at high elevations in the Cairngorm Mountains, Scotland.

737 *Geoderma*, 95, 1–14. [https://doi.org/10.1016/S0016-7061\(99\)00060-9](https://doi.org/10.1016/S0016-7061(99)00060-9)

738 Guisan, A., & Thuiller, W. (2005) Predicting species distribution: Offering more than simple habitat

739 models. *Ecology Letters*, 8, 993–1009. <https://doi.org/10.1111/j.1461-0248.2005.00792.x>

740 Haesen, S., Lembrechts, J. J., De Frenne, P., Lenoir, J., Aalto, J., Ashcroft, M. et al. (2021) ForestTemp

741 Sub-canopy microclimate temperatures of European forests. *Global Change Biology*, 27, 6307–  
742 6319. <https://doi.org/10.1111/gcb.15892>

743 Hartig, F. (2018) *Yes, statistical errors are slowing down scientific progress! Theoretical ecology*.  
744 Available at [https://theoreticalecology.wordpress.com/2018/05/03/yes-statistical-errors-are-](https://theoreticalecology.wordpress.com/2018/05/03/yes-statistical-errors-are-slowing-down-scientific-progress/)  
745 [slowing-down-scientific-progress/](https://theoreticalecology.wordpress.com/2018/05/03/yes-statistical-errors-are-slowing-down-scientific-progress/) [Accessed 2 November 2022]

746 Hartig, F. (2022) *DHARMA: Residual diagnostics for hierarchical (multi-level / mixed) regression*  
747 *Models. R package version 0.4.5*. Available at <https://CRAN.R-project.org/package=DHARMA>  
748 [Accessed 14 November 2021]

749 Hijmans, R. J., van Etten, J. (2012) *Raster: Geographic data analysis and modeling. R package version*  
750 *3.6-3*. Available at <http://CRAN.R-project.org/package=raster> [Accessed 5 October 2021]

751 Hooper, D. U., Adair, E. C., Cardinale, B. J., Byrnes, J. E. K., Hungate, B. A., Matulich, K. L. et al. (2012)  
752 A global synthesis reveals biodiversity loss as a major driver of ecosystem change. *Nature*, 486,  
753 105–108. <https://doi.org/10.1038/nature11118>

754 Howe, F., & Smallwood, J. (1982) Ecology of seed dispersal. *Annual Review of Ecology and Systematics*,  
755 13, 201–228. <https://doi.org/10.1146/annurev.es.13.110182.001221>

756 Hu, F. S., Higuera, P. E., Duffy, P., Chipman, M. L., Rocha, A. V., Young, A. M. et al. (2015) Arctic tundra  
757 fires: Natural variability and responses to climate change. *Frontiers in Ecology and the*  
758 *Environment*, 13, 369–377. <https://doi.org/10.1890/150063>

759 Jonasson, S. (1988) Evaluation of the point intercept method for the estimation of plant biomass.  
760 *Oikos*, 52, 101–106.

761 Jones, N. T., & Gilbert, B. (2016) Biotic forcing: the push–pull of plant ranges. *Plant Ecology*, 217, 1331–  
762 1344. <https://doi.org/10.1007/s11258-016-0603-z>

763 Kaarlejärvi, E., & Olofsson, J. (2014) Concurrent biotic interactions influence plant performance at  
764 their altitudinal distribution margins. *Oikos*, 123, 943–952. <https://doi.org/10.1111/oik.01261>

765 Karger, D. N., Conrad, O., Böhner, J., Kawohl, T., Kreft, H., Soria-Auza, R. W. et al. (2017) Climatologies  
766 at high resolution for the Earth land surface areas. *Scientific Data*, 4, 170122.  
767 <https://doi.org/10.1038/sdata.2017.122>

768 Keddy, P. A. (1992) Assembly and response rules: two goals for predictive community ecology. *Journal*  
769 *of vegetation science*, 3, 157–164. <https://doi.org/10.2307/3235676>

770 Keitt, T., Bivand, R., Pebesma, E. & Rowlingson, B. (2010) *rgdal: Bindings for the Geospatial Data*  
771 *Abstraction Library. Version 1.6-5*. Available at: <https://CRAN.R-project.org/package=rgdal>  
772 [Accessed 28 March 2023]

773 Klanderud, K. (2010) Species recruitment in alpine plant communities: The role of species interactions  
774 and productivity. *Journal of Ecology*, 98, 1128–1133. <https://doi.org/10.1111/j.1365-2745.2010.01703.x>

775

776 Kleyer, M., Bekker, R. M., Knevel, I. C., Bakker, J. P., Thompson, K., Sonnenschein, M. et al. (2008) The  
777 LEDA traitbase: a database of life- history traits of the northwest European flora. *Journal of*  
778 *Ecology*, 96, 1266–1274. <https://doi.org/10.1111/j.1365-2745.2008.01430.x>

779 Kopecký, M., Macek, M., & Wild, J. (2021) Science of the Total Environment Topographic Wetness  
780 Index calculation guidelines based on measured soil moisture and plant species composition.  
781 *Science of the Total Environment*, 757, 143785.  
782 <https://doi.org/10.1016/j.scitotenv.2020.143785>

783 Körner, C. (2021) *Alpine plant life: Functional plant ecology of high mountain ecosystems*, 3rd edition.  
784 Springer Nature Switzerland AG 2021. <https://doi.org/10.1007/978-3-030-59538-8>

785 Kullman, L. (2015) Recent and past trees and climates at the Arctic/Alpine margin in Swedish Lapland:  
786 An Abisko case study Review. *Journal of Biodiversity Management & Forestry*, 4, 1–12.  
787 doi:10.4172/2327-4417.1000150

788 Legendre P, Legendre J (1998) *Numerical Ecology*, 3rd edition. Elsevier, Amsterdam.



789 Lembrechts, J. J., Lenoir, J., Nuñez, M. A., Pauchard, A., Geron, C., Bussé, G. et al. (2018) Microclimate  
790 variability in alpine ecosystems as stepping stones for non-native plant establishment above  
791 their current elevational limit. *Ecography*, 41, 900–909. <https://doi.org/10.1111/ecog.03263>

792 Lembrechts, J. J., Lenoir, J., Roth, N., Hattab, T., Milbau, A., Haider, S. et al (2019) Comparing  
793 temperature data sources for use in species distribution models: From in-situ logging to  
794 remote sensing. *Global Ecology and Biogeography*, 28, 1578–1596.  
795 <https://doi.org/10.1111/geb.12974>

796 Lembrechts, J. J., Milbau, A., & Nijs, I. (2014) Alien roadside species more easily invade alpine than  
797 lowland plant communities in a subarctic mountain ecosystem. *PLoS ONE*, 9, 1–10.  
798 <https://doi.org/10.1371/journal.pone.0089664>

799 Lembrechts, J. J., Aalto, J., Ashcroft, M. B., De Frenne, P., Kopecký, M., Lenoir, J. et al. (2020) SoilTemp:  
800 A global database of near-surface temperature. *Global Change Biology*, 26, 6616–6629.  
801 <https://doi.org/10.1111/gcb.15123>

802 Lembrechts, J. J., van den Hoogen, J., Aalto, J., Ashcroft, M., De Frenne, P., Kemppinen, J. et al (2021)  
803 Global maps of soil temperature. *Global Change Biology*, 28, 3110–3144.  
804 <https://doi.org/10.1111/gcb.16060>

805 Lenoir, J., Gégout, J. C., Guisan, A., Vittoz, P., Wohlgemuth, T., Zimmermann, N. E. et al. (2010) Cross-  
806 scale analysis of the region effect on vascular plant species diversity in southern and northern  
807 European mountain ranges. *PLoS One*, 5, e15734.  
808 <https://doi.org/10.1371/journal.pone.0015734>

809 Lenth, R. (2022) *Emmeans: Estimated marginal means, aka least-squares means. Version 1.8.2.*  
810 Available at: <https://CRAN.R-project.org/package=emmeans> [Accessed 14 November 2021]

811 Leroy, B., Delsol, R., Hugué, B., Meynard, C. N., Barhoumi, C., Barbet-Massin, M., & Bellard, C. (2018)  
812 Without quality presence–absence data, discrimination metrics such as TSS can be misleading  
813 measures of model performance. *Journal of Biogeography*, 45, 1994–2002.  
814 <https://doi.org/10.1111/jbi.13402>

815 Lewis, R. J., de Bello, F., Bennett, J. A., Fibich, P., Finerty, G. E., Götzenberger, L. et al. (2017) Applying  
816 the dark diversity concept to nature conservation. *Conservation Biology*, 31, 40–47.  
817 <https://doi.org/10.1111/cobi.12723>

818 Lewis, R. J., Szava-Kovats, R., & Pärtel, M. (2016) Estimating dark diversity and species pools: An  
819 empirical assessment of two methods. *Methods in Ecology and Evolution*, 7, 104–113.  
820 <https://doi.org/10.1111/2041-210X.12443>

821 Lindén, E., Gough, L., & Olofsson, J. (2021) Large and small herbivores have strong effects on tundra  
822 vegetation in Scandinavia and Alaska. *Ecology and Evolution*, 11, 12141–12152.  
823 <https://doi.org/10.1002/ece3.7977>

824 Lüdecke, D., Ben-Shachar, M., Patil, I., Waggoner, P. & Makowski, D. (2021) “performance: An R  
825 package for assessment, comparison and testing of statistical models.” *Journal of Open Source*  
826 *Software*, 6, 3139. <https://doi.org/10.21105/joss.03139>

827 MacDougall, A. S., Caplat, P., Olofsson, J., Siewert, M. B., Bonner, C., Esch et al. (2021)  
828 Comparison of the distribution and phenology of Arctic Mountain plants between the early  
829 20th and 21st centuries. *Global Change Biology*, 27, 5070–5083.  
830 <https://doi.org/10.1111/gcb.15767>

831 Meyer, C., Weigelt, P., & Kreft, H. (2016) Multidimensional biases, gaps and uncertainties in global  
832 plant occurrence information. *Ecology Letters*, 19, 992–1006.  
833 <https://doi.org/10.1111/ele.12624>

834 Moeslund, J. E., Brunbjerg, A. K., Clausen, K. K., Dalby, L., Fløjgaard, C., Juel, A., & Lenoir, J. (2017)  
835 Using dark diversity and plant characteristics to guide conservation and restoration. *Journal of*  
836 *Applied Ecology*, 54, 1730–1741. <https://doi.org/10.1111/1365-2664.12867>

837 Mohd, M. H., Murray, R., Plank, M. J., & Godsoe, W. (2016). Effects of dispersal and stochasticity on  
838 the presence–absence of multiple species. *Ecological Modelling*, 342, 49–59.  
839 <https://doi.org/10.1016/j.ecolmodel.2016.09.026>

840 Mooney, H., Larigauderie, A., Cesario, M., Elmquist, T., Hoegh-Guldberg, O., Lavorel, S. et al. (2009)  
841 Biodiversity, climate change, and ecosystem services. *Current Opinion in Environmental*  
842 *Sustainability*, 1, 46–54. <https://doi.org/10.1016/j.cosust.2009.07.006>

843 Mossberg, B. & Stenberg, L. (2008) *Fjällflora: Sverige, Finland, Norge, Svalbard*. Wahlström &  
844 Widstrand.

845 Newbold, T., Hudson, L. N., Hill, S. L. L., Contu, S., Lysenko, I., Senior, R. A. et al. (2015) Global effects  
846 of land use on local terrestrial biodiversity. *Nature*, 520, 45–50.  
847 <https://doi.org/10.1038/nature14324>

848 Oksanen, J., Blanchet, F.G., Kindt, R. et al. (2022) *Vegan: Community ecology package. Version 2.6-4*.  
849 Available at: <https://CRAN.R-project.org/package=vegan> [Accessed 2 November 2022]

850 Olofsson, J. (2001) Influence of herbivory and abiotic factors on the distribution of tall forbs along a  
851 productivity gradient: A transplantation experiment. *Oikos*, 94, 351–357.  
852 <https://doi.org/10.1034/j.1600-0706.2001.940216.x>

853 Ozinga, W. A., Hennekens, S. M., Schaminée, J. H. J., Bekker, R. M., Prinzing, A., Bonn, S. et al. (2005)  
854 Assessing the relative importance of dispersal in plant communities using an ecoinformatics  
855 approach. *Folia Geobotanica*, 40, 53–67. <https://doi.org/10.1007/BF02803044>

856 Parolo, G., Rossi, G., & Ferrarini, A. (2008). Toward improved species niche modelling: *Arnica montana*  
857 in the Alps as a case study. *Journal of Applied Ecology*, 45, 1410–1418.  
858 <https://doi.org/10.1111/j.1365-2664.2008.01516.x>

859 Pärtel, M. (2014) Community ecology of absent species: Hidden and dark diversity. *Journal of*  
860 *Vegetation Science*, 25, 1154–1159. <https://doi.org/10.1111/jvs.12169>

861 Pärtel, M., Carmona, C. P., Zobel, M., Moora, M., Riibak, K., & Tamme, R. (2019) DarkDivNet – A global  
862 research collaboration to explore the dark diversity of plant communities. *Journal of*  
863 *Vegetation Science*, 30, 1039–1043. <https://doi.org/10.1111/jvs.12798>

864 Pärtel, M., Szava-Kovats, R., & Zobel, M. (2011) Dark diversity: Shedding light on absent species. *Trends*  
865 *in Ecology and Evolution*, 26, 124–128. <https://doi.org/10.1016/j.tree.2010.12.004>

866 Pärtel, M., Szava-Kovats, R., & Zobel, M. (2013) Community completeness: Linking local and dark  
867 diversity within the species pool concept. *Folia Geobotanica*, 48, 307–317.  
868 <https://doi.org/10.1007/s12224-013-9169-x>

869 Pebesma, E. J., Bivand, R. S. (2005) Classes and methods for spatial data in R. *R news*, 5, 9–13.

870 Pellissier, L., Bräthen, K. A., Pottier, J., Randin, C. F., Vittoz, P., Dubuis, A. et al. (2010) Species  
871 distribution models reveal apparent competitive and facilitative effects of a dominant species  
872 on the distribution of tundra plants. *Ecography*, 33, 1004–1014.  
873 <https://doi.org/10.1111/j.1600-0587.2010.06386.x>

874 Pollock, L. J., Tingley, R., Morris, W. K., Golding, N., O'Hara, R. B., Parris, K. M. et al. (2014)  
875 Understanding co-occurrence by modelling species simultaneously with a Joint Species  
876 Distribution Model (JSDM). *Methods in Ecology and Evolution*, 5, 397–406.  
877 <https://doi.org/10.1111/2041-210X.12180>

878 Prieur-Richard, A. H., & Lavorel, S. (2000) Invasions: The perspective of diverse plant communities.  
879 *Austral Ecology*, 25, 1–7. <https://doi.org/10.1046/j.1442-9993.2000.01033.x>

880 QGIS.org, 2021. QGIS Geographic Information System. QGIS Association. Available at:  
881 <http://www.qgis.org>

882 Quinn, Q. P., Keough, M. J. (2002) *Experimental design and data analysis for biologists*. Cambridge  
883 University Press, Cambridge. <https://doi.org/10.1017/CBO9780511806384>

884 R Core Team (2021) R: A language and environment for statistical computing. R Foundation for

885           Statistical Computing, Vienna, Austria. Available at: <https://www.R-project.org/>

886 Rashid, I., Haq, S. M., Lembrechts, J. J., Khuroo, A. A., Pauchard, A., & Dukes, J. S. (2021) Railways  
887 redistribute plant species in mountain landscapes. *Journal of Applied Ecology*, 58, 1967–1980.  
888 <https://doi.org/10.1111/1365-2664.13961>

889 Riibak, K., Reitalu, T., Tamme, R., Helm, A., Gerhold, P., Znamenskiy, S. et al. (2015) Dark diversity in  
890 dry calcareous grasslands is determined by dispersal ability and stress-tolerance. *Ecography*,  
891 38, 713–721. <https://doi.org/10.1111/ecog.01312>

892 Sonesson, M., & Lundberg, B. (1974) Late Quaternary forest development of the Tornetrask area,  
893 North Sweden. *Oikos*, 25, 121–133. <https://doi.org/10.2307/3543947>

894 Soudzilovskaia, N. A., Vaessen, S., Barcelo, M., He, J., Rahimlou, S., Abarenkov, K. et al. (2020)  
895 FungalRoot: global online database of plant mycorrhizal associations. *New Phytologist*, 227,  
896 955–966. <https://doi.org/10.1111/nph.16569>

897 Stephenson, I. (2016) *What is Dark Diversity?* Methods blog. Available at  
898 <https://methodsblog.com/2016/05/22/dark-diversity/> [Accessed 4 April 2022]

899 Sugihara, N. G., Van Wagtenonk, J. W., & Fites-Kaufman, J. (2006) Fire as an ecological process. In:  
900 Van Wagtenonk, J. W., Sugihara, N. G., Stephens, S. L., Thode, A. E., Shaffer, K. E., & Fites-  
901 Kaufman, J. A. (Eds), *Fire in California's ecosystems*, 1st edition. University of California Press,  
902 pp. 58-74.

903 Tendersoo, L. (Ed) (2017) *Biogeography of Mycorrhizal Symbiosis*, 1st edition. Springer International  
904 Publishing 2017. <https://doi.org/10.1007/978-3-319-56363-3>

905 Tessarolo, G., Rangel, T. F., Araújo, M. B., & Hortal, J. (2014) Uncertainty associated with survey design  
906 in Species Distribution Models. *Diversity and Distributions*, 20, 1258–1269.  
907 <https://doi.org/10.1111/ddi.12236>

908 Tilman, D., Isbell, F., & Cowles, J. M. (2014) Biodiversity and ecosystem functioning. *Annual Review of*  
909 *Ecology, Evolution, and Systematics*, 45, 471–493. <https://doi.org/10.1146/annurev-ecolsys-120213-091917>

911 Trindade, D. P., Carmona, C. P., Reitalu, T., & Pärtel, M. (2023) Observed and dark diversity dynamics  
912 over millennial time scales: fast life-history traits linked to expansion lags of plants in northern  
913 Europe. *Proceedings of the Royal Society B*, 290, 20221904.  
914 <https://doi.org/10.1098/rspb.2022.1904>

915 Tybirk, K., Nilsson, M. C., Michelsen, A., Kristensen, H. L., Sheytsova, A., Strandberg, M. T. et al. (2000)  
916 Nordic *Empetrum* dominated ecosystems: Function and susceptibility to environmental  
917 changes. *Ambio*, 29, 90–97. <https://doi.org/10.1579/0044-7447-29.2.90>

918 Vonlanthen, C. M., Kammer, P. M., Eugster, W., Bühler, A., & Veit, H. (2006) Alpine vascular plant  
919 species richness: The importance of daily maximum temperature and pH. *Plant Ecology*, 184,  
920 13–25. <https://doi.org/10.1007/s11258-005-9048-5>

921 Wedegärtner, R. E., Lembrechts, J. J., van der Wal, R., Barros, A., Chauvin, A., Janssens et al. (2022)  
922 Hiking trails shift plant species' realized climatic niches and locally increase species richness.  
923 *Diversity and Distributions*, 28, 1416-1429 <https://doi.org/10.1111/ddi.13552>

924 Westoby, M. (1998) A leaf-height-seed (LHS) plant ecology strategy scheme. *Plant and Soil*, 199, 213–  
925 227. <https://doi.org/10.1023/A:1004327224729>

926 Wiegmans, D., Larson, K., Clavel, J., Spreeuwes, J., Pirée, A., Nijs, I., & Lembrechts, J. (2023) Historic  
927 disturbance events may overrule climatic factors as drivers of ruderal species distributions in  
928 the Scandinavian mountains. *Authorea Preprints*. 10.22541/au.167515746.69858832/v1

929 Wunderlich, R. F., Lin, Y. P., Anthony, J., & Petway, J. R. (2019) Two alternative evaluation metrics to  
930 replace the true skill statistic in the assessment of species distribution models. *Nature*  
931 *Conservation*, 35, 97-116.

932

933	<b>Appendices</b>
934	Appendix S1. Details online data collection
935	Appendix S2. Additional results
936	Appendix S3. Contrast tests mycorrhizal associations